Dynamic Event-Triggered $\mathcal{H}_\infty$ Load Frequency Control for Multi-Area Power Systems Subject to Hybrid Cyber Attacks

Jing Wang, Dongji Wang, Lei Su, Ju H. Park, *Senior Member, IEEE*, and Hao Shen, *Member, IEEE*

***Abstract*—This article aims at designing a dynamic event-triggered $\mathcal{H}_\infty$ load frequency controller for multi-area power systems affected by false data-injection attacks and denial-of-service attacks. A dynamic event-triggered scheme, whose threshold parameter varies with objective system states, is employed to make rational use of limited network bandwidth resources and improve the efficiency of the data utilization. Then, taking the impacts of the aforementioned hybrid cyber attacks into consideration, an attractive system model is established. Whereafter, several sufficient conditions, which can guarantee the exponential mean-square stability with a preset $\mathcal{H}_\infty$ performance index of the studied system, are obtained through utilizing Lyapunov stability theory. Additionally, the desired controller is designed via handling convex optimization problems. Finally, a simulation example is displayed to explain the validity of the proposed method.**

***Index Terms*—Dynamic event-triggered scheme, hybrid cyber attacks, load frequency control, multi-area power systems.**

I. Introduction

With the appearance of power systems, electric energy, which possesses the characteristics of high efficiency, nonpollution, and convenience for controlling, has been extensively applied in our daily life [1], [2]. For making interconnected power systems work normally, it is of great significance to match the total power generation with the load demand. It is worth mentioning that the load frequency control (LFC), whose primary objective is to keep the frequency and power exchanges between areas maintaining the scheduled values to supply high-quality electric energy, has been proved to be fairly valid in the control of power systems [3]–[5]. Notice that the traditional LFC, transmitting data through the dedicated communication channel, is no longer suitable for power systems with expanding scale due to its poor flexibility and higher maintenance cost; while LFC based on an open communication network (OCN) has been widely used in modern power systems.

Nevertheless, the introduction of OCN is accompanied by the network-induced phenomena which cannot be ignored, e.g., time delays. Naturally, the past few decades have witnessed an enormous amount of reports on LFC for time-delayed power systems [6]–[8]. To name but a few key ones, the problem of delay-dependent stability for LFC with both fixed and time-varying delays was discussed by Jiang *et al.* [9]. Sönmez *et al.* [10] put forward an analytical method for determining delay margins, and also solved out an upper bound of time delays for the stability of power systems. Besides the phenomenon of time delays, the potential cyber attacks, which can bring a certain degree of damage to the stability of power systems, may also take place in the process of the data transmission. In general, cyber attacks can fall into two main categories, to be specific, false data-injection (FDI) attacks and denial-of-service (DoS) attacks [11]–[14].

It is worth noting that DoS attacks can destroy the availability of data by blocking the transmission channels, and result in packet losses. As for FDI attacks, the attackers attempt to inject false information into communication channels to destroy the output of the measurement, such that the trustworthiness of data can be influenced. Therefore, as one of the hottest topics in the field of security control, cyber-security has stimulated the research interest of many scholars. For instance, in [15], the stability analysis for networked control systems (NCSs) was studied with DoS attacks, where the packet loss resulted from DoS attacks was assumed to obey the Bernoulli distribution. In [16], a resilient event-triggered H_∞ LFC method for power systems subject to DoS attacks was investigated. In [17], with regard to the influence of FDI attacks, the authors proposed a security distributed LFC scheme based on credibility to keep the stable operation of power systems. Note

Manuscript received 10 February 2022; accepted 26 March 2022. Date of publication 11 April 2022; date of current version 18 November 2022. This work was supported in part by the National Natural Science Foundation of China under Grant 62173001, Grant 61873002, Grant 61703004, and Grant 61973199; in part by the Major Natural Science Foundation of Higher Education Institutions of Anhui Province under Grant KJ2020ZD28; in part by the Natural Science Foundation for Excellent Young Scholars of Anhui Province under Grant 2108085Y21; in part by the Major Technologies Research and Development Special Program of Anhui Province under Grant 202003a05020001; and in part by the Key Research and Development Projects of Anhui Province under Grant 202104a05020015. This work of Ju H. Park was supported by the National Research Foundation of Korea (NRF) Grant funded by the Korea Government (MSIT) under Grant 2020R1A2B5B02002002. This article was recommended by Associate Editor D. Yue. *(Corresponding authors: Ju H. Park; Hao Shen.)*

Jing Wang, Dongji Wang, Lei Su, and Hao Shen are with the School of Electrical and Information Engineering and the Anhui Provincial Key Laboratory of Power Electronics and Motion Control, Anhui University of Technology, Ma'anshan 243032, China (e-mail: jingwang08@126.com; dongjiwang2019@gmail.com; leisu2015@gmail.com; haoshen10@gmail.com).

Ju H. Park is with the Department of Electrical Engineering, Yeungnam University, Kyongsan 38541, Republic of Korea (e-mail: jessie@ynu.ac.kr).

Color versions of one or more figures in this article are available at https://doi.org/10.1109/TSMC.2022.3163261.

Digital Object Identifier 10.1109/TSMC.2022.3163261

that malicious cyber attacks, which aim at different systems, such as NCSs [18], and cyber–physical systems [19]–[21], have been given a full consideration. Nevertheless, the security issues of multi-area power systems with regard to hybrid cyber attacks have not been adequately studied, which is one of the motivations for us to further research.

Furthermore, another point worth noting is that owing to the limited bandwidth resources, the excessive data transmission may lead to the communication channel congestion. Fortunately, the event-triggered transmission scheme (ETTS), which can reduce transmission burdens and rationally use the limited bandwidth resources, has gained increasing concerns [22]–[26]. For example, in [27], an ETTS based on sampled data was proposed to reduce the amount of redundant data. The event-based guaranteeing cost control issue of Markov jump discrete-time neural networks with fading channels and distributed delays was investigated in [28]. The aforementioned ETTSs, whose threshold parameters are fixed constants and cannot easily make an appropriate selection in advance, are called static ETTSs. For eliminating the limitations of static ETTSs, an improved ETTS with a sampler and a dynamic threshold parameter was proposed in [29] to use the network resources reasonably and prevent unnecessary continuous monitoring of nonlinear multiagent systems. What needs to be pointed out is that although substantial ETTS results have been applied to multifarious NCSs, little attention has been paid to designing appropriate ETTSs under the impact of inevitable hybrid cyber attacks, let alone dynamic ETTSs, particularly for multi-area power systems, which is another motivation for our current investigation.

Based on the above-mentioned discussions, the problem of dynamic ETTS $\mathcal{H}_\infty$ LFC for multi-area power systems subject to DoS attacks and FDI attacks is studied in the work. The primary highlights of our paper are summarized in the following.

1) Inspired by [29], a dynamic ETTS, whose threshold parameter appropriately changes with the fluctuation of the resulting system states, is adopted for handling the LFC problem of multi-area power systems in this article. Moreover, the conclusion that the dynamic ETTS is more effective than the static one in the same case can be drawn from the obtained research results.
2) Different from [30] which uses the static ETTS and considers the DoS and deception attacks, this article utilizes a dynamic ETTS and considers the hybrid cyber attacks, including both DoS attacks and another type of cyber attacks, FDI attacks. Besides, by considering the dynamic ETTS under the presence of DoS attacks as well as FDI attacks, an attractive system model is established.
3) Taking the built system model into account, by utilizing the Lyapunov stability theory, the exponential stability in the sense of mean-square at an $\mathcal{H}_\infty$ performance level for the resulting systems is guaranteed.

The remainder of this article is organized below. In Section II, the system model for the multi-area LFC scheme is established in consideration of a dynamic ETTS under DoS attacks and FDI attacks. The main results of this article, in

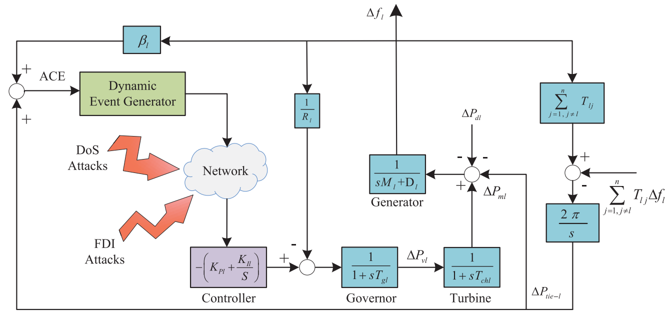

Fig. 1. Diagram of the lth control area of LFC power systems with a dynamic ETTS subject to hybrid cyber attacks.

TABLE I
EXPLANATIONS OF TERMINOLOGIES

Terminologies	Explanations
ΔP_{dl}	the deviation of the lth area load
T_{chl}	the time constant of the lth area turbine
ΔP_{vl}	the deviation of the lth area position
Δf_l	the deviation of the lth area frequency
T_{gl}	the time constant of the lth area governor
ΔP_{tie-l}	the deviation of the lth area tie-line active power
M_l	the rotational inertia of the lth area generator
R_l	the speed drop coefficient of the lth area governor
ΔP_{ml}	the deviation of the lth area generator mechanical output
D_l	the damping coefficient of the lth area generator

Section III, are presented. Moreover, Section IV provides a simulation example, indicating the availability of the method proposed in this work. Finally, Section V is provided to summarize the conclusion.

Notations: The used notations in this article are standard and the corresponding explanations are presented in the following. $\|\cdot\|$ stands for Euclidean norm; diag$\{\cdots\}$ is block-diagonal matrix; sup$\{\cdot\}$ is minimum upper bound; $\lambda_{\min}\{A\}(\lambda_{\max}\{A\})$ means the smallest (largest) eigenvalue of matrix A; $\mathbb{E}\{\cdots\}$ is the mathematical expectation; $*$ defines entry caused by the symmetry; C^{T} is the transposition of matrix C; $A > 0$ is symmetric positive definite matrix; $\mathcal{R}_{>0}$ expresses set of reals larger than 0; sym$\{B\}$ is symmetrized expression of $B + B^{\mathrm{T}}$; I is identity matrix with suitable dimensions; $\mathcal{N}_{>0}$ means set of natural numbers larger than 0; and $\mathcal{L}_2[0, \infty)$ is space of square-summable infinite vector sequences on $[0, \infty)$.

II. System Description

A. System Framework of Multi-Area LFC Model With Communication Networks

All power generation units can be simplified into an equivalent one in each control area and the framework of the lth control area of LFC power systems is described in Fig. 1 [16]. The dynamic model for multi-area power systems with different system parameters listed in Table I is

$$\begin{cases} \dot{x}(t) = \mathcal{A}x(t) + \mathcal{B}u(t) + \mathcal{F}\omega(t) \\ y(t) = \mathcal{C}x(t) \end{cases} \tag{1}$$

where

$$y_l(t) = \begin{bmatrix} ACE_l & \int ACE_l \end{bmatrix}^T$$
$$x(t) = \begin{bmatrix} x_1^T(t) & x_2^T(t) & \cdots & x_n^T(t) \end{bmatrix}^T$$

$$y(t) = \begin{bmatrix} y_1^T(t) & y_2^T(t) & \cdots & y_n^T(t) \end{bmatrix}^T$$
$$u(t) = \begin{bmatrix} u_1^T(t) & u_2^T(t) & \cdots & u_n^T(t) \end{bmatrix}^T$$
$$\omega(t) = \begin{bmatrix} \Delta P_{d1}(t) & \Delta P_{d2}(t) & \cdots & \Delta P_{dn}(t) \end{bmatrix}^T$$
$$x_l(t) = \begin{bmatrix} \Delta f_l & \Delta P_{\text{tie}-l} & \Delta P_{ml} & \Delta P_{vl} & \int ACE_l \end{bmatrix}^T$$

with

$$\mathcal{A} = \begin{bmatrix} \mathcal{A}_{11} & \mathcal{A}_{12} & \cdots & \mathcal{A}_{1n} \\ \mathcal{A}_{21} & \mathcal{A}_{22} & \cdots & \mathcal{A}_{2n} \\ \vdots & \vdots & \ddots & \vdots \\ \mathcal{A}_{n1} & \mathcal{A}_{n2} & \cdots & \mathcal{A}_{nn} \end{bmatrix}$$

$$\mathcal{A}_{lk} = \begin{bmatrix} 0 & 0 & 0 & 0 & 0 \\ -2\pi T_{lk} & 0 & 0 & 0 & 0 \\ 0 & 0 & 0 & 0 & 0 \\ 0 & 0 & 0 & 0 & 0 \\ 0 & 0 & 0 & 0 & 0 \end{bmatrix}, \mathcal{C}_l = \begin{bmatrix} \beta_l & 0 \\ 1 & 0 \\ 0 & 0 \\ 0 & 0 \\ 0 & 1 \end{bmatrix}^T$$

$$\mathcal{A}_{ll} = \begin{bmatrix} -\frac{D_l}{M_l} & -\frac{1}{M_l} & \frac{1}{M_l} & 0 & 0 \\ 2\pi \sum\limits_{k=1,k\neq l}^{n} T_{lk} & 0 & 0 & 0 & 0 \\ 0 & 0 & -\frac{1}{T_{chl}} & \frac{1}{T_{chl}} & 0 \\ -\frac{1}{R_l T_{gl}} & 0 & 0 & -\frac{1}{T_{gl}} & 0 \\ \beta_l & 1 & 0 & 0 & 0 \end{bmatrix}$$

$$\mathcal{B}_l = \begin{bmatrix} 0 & 0 & 0 & \frac{1}{T_{gl}} & 0 \end{bmatrix}^T, \mathcal{B} = \text{diag}\{\mathcal{B}_1, \mathcal{B}_2, \ldots, \mathcal{B}_n\}$$
$$\mathcal{F}_l = \begin{bmatrix} -\frac{1}{M_l} & 0 & 0 & 0 & 0 \end{bmatrix}^T, \mathcal{F} = \text{diag}\{\mathcal{F}_1, \mathcal{F}_2, \ldots, \mathcal{F}_n\}$$
$$\mathcal{C} = \text{diag}\{\mathcal{C}_1, \mathcal{C}_2, \ldots, \mathcal{C}_n\}, T_{lk} = T_{kl}.$$

The signal of area control error (ACE) for each area, which is deemed as a linear combination of the frequency deviation and the tie-line power exchange between areas, can be described as follows:

$$ACE_l = \beta_l \Delta f_l + \Delta P_{\text{tie}-l} \tag{2}$$

where β_l represents the frequency deviation factor in the lth control area, and the tie-line active power deviation satisfies the following equality:

$$\sum_{l=1}^{n} \Delta P_{\text{tie}-l} = 0.$$

In this article, a kind of proportional-integral (PI) controller for multi-area LFC scheme is designed. Assume that ACE signal is sent to the PI controller over an OCN. Then, using the ACE signal as the desired controller input, the lth control area of the PI controller is designed as

$$u_l(t) = -K_{Pl} ACE_l - K_{Il} \int ACE_l \tag{3}$$

where K_{Pl} and K_{Il} represent the proportional and integral gains of the lth area, respectively.

Combining (1) with (3), the designed PI controller of the multi-area LFC scheme is formulated below

$$u(t) = -Ky(t) \tag{4}$$

where $K = \text{diag}\{K_1, K_2, \ldots, K_n\}$, $K_l = \begin{bmatrix} K_{Pl} \; K_{Il} \end{bmatrix}$, $l \in \{1, 2, \ldots, n\}$.

B. Dynamic ETTS With DoS Attacks

In this section, under the existence of DoS attacks, a dynamic ETTS is introduced to save network communication resources. Assume that DoS attacks are periodic jamming signals with power constraint [30], satisfying the condition given as follows:

$$\mathcal{I}_{\text{DoS}}(t) = \begin{cases} 0, \ t \in \big[(p-1)\mathcal{T}, (p-1)\mathcal{T} + \mathcal{T}_{\text{off}}\big) \\ 1, \ t \in \big[(p-1)\mathcal{T} + \mathcal{T}_{\text{off}}, p\mathcal{T}\big) \end{cases} \tag{5}$$

where $\mathcal{T} \in \mathcal{R}_{>0}$ is the period of the jammer signal and $\mathcal{T}_{\text{off}} < \mathcal{T}$; $p \in \mathcal{N}_{>0}$ denotes the period number. Therefore, during one period, the interval $[0, \mathcal{T}_{\text{off}})$ stands for the sleeping time of DoS attacks, while the interval $[\mathcal{T}_{\text{off}}, \mathcal{T})$ denotes the active time of DoS attacks. That is to say, the measurement data can be transmitted successfully in intervals $[(p-1)\mathcal{T}, (p-1)\mathcal{T} + \mathcal{T}_{\text{off}})$ while denied within intervals $[(p-1)\mathcal{T} + \mathcal{T}_{\text{off}}, p\mathcal{T})$.

Without the consideration of DoS attacks, the dynamic ETTS is described as

$$e^T(t)\mathcal{C}^T \Omega \mathcal{C} e(t) < \tilde{\Psi}(t) x^T(t_r h + qh)\mathcal{C}^T \Omega \mathcal{C} x(t_r h + qh) \tag{6}$$

where $\tilde{\Psi}(t) = \eta(1 - \alpha \tanh(e^T(t)e(t) - \tilde{\theta}))$, and η is a basic threshold scalar; $\tilde{\Psi}(t)$ denotes the real parameter of the dynamic threshold; $\alpha > 0$ represents the degree of the variability of η; $(e^T(t)e(t) - \tilde{\theta})$ determines the direction of the variability of η, and $\tilde{\theta} > 0$; $e(t) = x(t_r h) - x(t_r h + qh)$, $x(t_r h)$ and $x(t_r h + qh)$ represent the latest transmitted data and the currently sampled data, respectively; h is the sampling period; $\Omega = \text{diag}\{\Omega_1, \Omega_2, \ldots, \Omega_n\} > 0$ is a weight matrix to be designed; and $q \in \mathcal{N}_{>0}$ is the number of sampling periods.

Remark 1: In order to utilize the network resources rationally, the ETTS has attracted extensive attention of numerous scholars. Note that the threshold parameter of the ETTS plays a vital role in the process of data transmission, while how to choose a suitable threshold parameter is quite difficult. Fortunately, inspired by [29], we choose dynamic ETTS (6) whose threshold parameter changes with the state variables of the resulting system but is not monotonous. In this article, $\eta(1 - \alpha \tanh(e^T(t)e(t) - \tilde{\theta}))$, as the real parameter of the dynamic threshold related to a time-varying term $(1 - \alpha \tanh(e^T(t)e(t) - \tilde{\theta}))$, is taken into account.

Remark 2: In view of the tendency of function $\tanh(x)$, when $e(t)$ is smaller than $\tilde{\theta}$, the real threshold parameter will be larger such that fewer data packages can be transmitted; on the contrary, when $e(t)$ is larger than $\tilde{\theta}$, the real threshold parameter will be smaller so that more data packages can be transmitted. As is well known, the stability conditions are derived on the basis of the pregiven dynamic event-triggered condition. But, it actually brings some challenges to solve these conditions because of the time-varying dynamic ETTS. Fortunately, the boundedness of $\tanh(x)$ function is considered to make appropriate scaling of the triggering condition, which is presented in the proof part of Theorem 1. Afterwards, some stability conditions are deduced, which are time independent and can make less calculation in the process of seeking solutions. At the same time, the monotonicity of the function $\tanh(x)$ can be utilized to make the proper evolution of dynamic parameters to a certain degree.

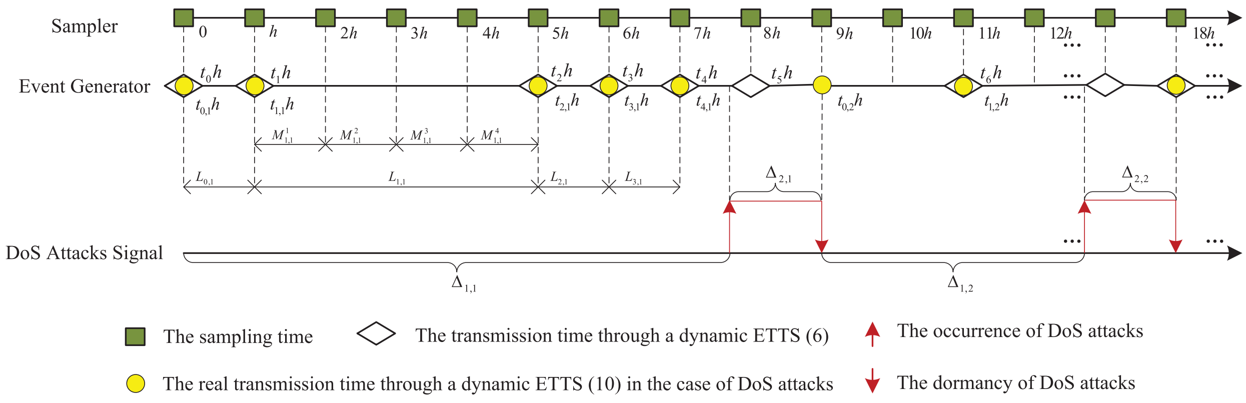

Fig. 2. Schematic diagram of the data transmission based on the dynamic ETTS in the case of DoS attacks with $\nu_{1,1} = 3$.

Remark 3: The operation mechanism of the given triggering condition is that if dynamic ETTS (6) is satisfied, the currently sampled data will be discarded directly; otherwise, they are transmitted immediately.

Remark 4: Under the condition of $\alpha = 0$, the designed dynamic ETTS (6) will be converted to a static one as shown in [31]–[33]. In addition, dynamic ETTS (6) can be regarded as a time-triggered scheme when $\eta = 0$. Furthermore, the real threshold parameter $\eta(1 - \alpha \tanh(e^T(t)e(t) - \tilde{\theta}))$ may be less than 0 if the value of α is too large, which makes condition (6) be also regarded as a time-triggered scheme due to the immediate transmission of currently sampled data.

When considering the impact of DoS attacks, the dynamic ETTS (6) is modified as follows:

$$t_{r+1}h = t_r h + \min_{q \in \mathcal{N}_{>0}} \Big\{ qh | e^T(t)\mathcal{C}^T \Omega \mathcal{C} e(t) \geq \tilde{\Psi}(t) x^T(t_r h + qh)\mathcal{C}^T \Omega \mathcal{C} x(t_r h + qh) \Big\} \quad (7)$$

where $t_{r+1}h \in [(p-1)\mathcal{T}, (p-1)\mathcal{T} + \mathcal{T}_{\text{off}})$ is the next transmitted time. Based on condition (7), the actually transmitted data is obtained as

$$y(t_{r,p}h) = \mathcal{C}x(t_{r,p}h) \quad (8)$$

where $r(p) = \sup\{r \in \mathcal{N} | t_{r,p}h \leq (p-1)\mathcal{T} + \mathcal{T}_{\text{off}}.\}$ and $r \in \{0, 1, \ldots, r(p)\}$, particularly, $t_{0,p}h = (p-1)\mathcal{T}$ with $h < \mathcal{T}$. In order to expediently analyze and understand, an example of the data transmission through the dynamic ETTS in the case of DoS attacks is described in Fig. 2 [30]. Moreover, for the sake of simplifying the notation, the event-triggered interval $L_{r,p} \triangleq [t_{r,p}h, t_{r+1,p}h)$ can be divided into the following subintervals:

$$L_{r,p} \triangleq \Big\{ \cup_{w=1}^{\nu_{r,p}} M_{r,p}^w \Big\} \cup M_{r,p}^{\nu_{r,p}+1}$$

where

$$\begin{aligned} M_{r,p}^w &\triangleq \big[t_{r,p}h + (w-1)h, t_{r,p}h + wh\big) \\ M_{r,p}^{\nu_{r,p}+1} &\triangleq \big[t_{r,p}h + \nu_{r,p}h, t_{r+1,p}h\big) \\ \nu_{r,p} &\triangleq \sup\big\{ w \in \mathcal{N}_{>0} | t_{r,p}h + wh < t_{r+1,p}h \big\}. \end{aligned}$$

Therefore, one can deduce the following equality:

$$\Delta_{1,p} = \cup_{r=0}^{r(p)} \cup_{w=1}^{\nu_{r,p}+1} \Big\{ M_{r,p}^w \cap \Delta_{1,p} \Big\}.$$

Now, for any $r \in \{0, 1, \ldots, r(p)\}$, the definitions of two piecewise functions are

$$\mu_{r,p}(t) \triangleq \begin{cases} t - t_{r,p}h, & t \in M_{r,p}^1 \cap \Delta_{1,p} \\ t - t_{r,p}h - h, & t \in M_{r,p}^2 \cap \Delta_{1,p} \\ \vdots \\ t - t_{r,p}h - \nu_{r,p}h, & t \in M_{r,p}^{\nu_{r,p}+1} \cap \Delta_{1,p} \end{cases}$$

$$e_{r,p}(t) \triangleq \begin{cases} 0, & t \in M_{r,p}^1 \cap \Delta_{1,p} \\ x(t_{r,p}h) - x(t_{r,p}h + h), & t \in M_{r,p}^2 \cap \Delta_{1,p} \\ \vdots \\ x(t_{r,p}h) - x(t_{r,p}h + \nu_{r,p}h), & t \in M_{r,p}^{\nu_{r,p}+1} \cap \Delta_{1,p} \end{cases}$$

where $\mu_{r,p}(t) \in (0, d_M)$ and $t \in L_{r,p} \cap \Delta_{1,p}$.

Then, combining the two piecewise functions defined above, equality (8) can be reformulated into the following form:

$$y(t_{r,p}h) = \mathcal{C}\big(e_{r,p}(t) + x(t - \mu_{r,p}(t))\big), t \in L_{r,p} \cap \Delta_{1,p} \quad (9)$$

and for $t \in L_{r,p} \cap \Delta_{1,p}$, the dynamic event-triggered condition (6) under DoS attacks is rewritten as

$$e_{r,p}^T(t)\mathcal{C}^T \Omega \mathcal{C} e_{r,p}(t) < \Psi(t) x^T\big(t - \mu_{r,p}(t)\big)\mathcal{C}^T \Omega \mathcal{C} x\big(t - \mu_{r,p}(t)\big) \quad (10)$$

where $\Psi(t) = \eta(1 - \alpha \tanh(e_{r,p}^T(t)e_{r,p}(t) - \tilde{\theta}))$.

C. False Data-Injection Attacks

In this section, we consider that FDI attacks take place under the precondition that DoS attacks are in the dormant time. As shown in Fig. 1, false signals are injected into the communication channel between the event generator and the PI controller, which can alter the measurement outputs so as to do severe damage to the data integrity. Under the dynamic ETTS with the presence of FDI attacks, the real measurement outputs [12] transmitted to the PI controller can be modeled as

$$\tilde{y}(t_{r,p}h) = y(t_{r,p}h) + \Gamma^y(t_{r,p}h)\kappa^y(t_{r,p}h)$$

where $\kappa^y(t_{r,p}h)$ represents the bounded energy false signals with arbitrariness; $\Gamma^y(t_{r,p}h) \in \{0, 1\}$ is the decidable variable of the attacker which obeys the Bernoulli distribution with the expectation $\mathbb{E}\{\Gamma^y(t_{r,p}h)\} = \bar{\tau}$ and variance $\mathbb{E}\{(\Gamma^y(t_{r,p}h) - \bar{\tau})^2\} = \sigma^2$. Note that $\Gamma^y(t_{r,p}h) = 0$ implies the currently sampled data can be sent to the PI controller without any hindrance, while $\Gamma^y(t_{r,p}h) = 1$ indicates that FDI attacks occur in the transmission process, causing the change of actual measurement outputs. For analyzing the impacts of FDI attacks and making calculations easily, an assumption will be provided later.

Remark 5: According to [34] and the references therein, it is not difficult to know that there are three ways to manipulate the measured values of the studied system under the presence of FDI attacks, namely, compromising the instruments on site, intercepting or tampering with those data packages when sent to the control center, and revising the control center database. In this article, only tampering with the data packages during the transmission to the PI controller is taken into account, and others will be considered in future studies.

Subsequently, on the basis of the dynamic ETTS under the aforementioned two types of cyber attacks, the actual input of the PI controller is

$$u(t) = \begin{cases} -K\big(\mathcal{C}e_{r,p}(t) + \mathcal{C}x\big(t - \mu_{r,p}(t)\big)\big) \\ -K\Gamma^y\big(t_{r,p}h\big)\kappa^y\big(t_{r,p}h\big),\ t \in L_{r,p} \cap \Delta_{1,p} \\ 0,\ t \in \Delta_{2,p}. \end{cases} \tag{11}$$

Remark 6: In this work, data transmission is realized through an OCN which is subject to FDI and DoS attacks. If DoS attacks do not occur, the process of data transmission can be carried out normally with the random occurrence of FDI attacks, then the update of the controller is realizable, namely, $u(t) = -K(\mathcal{C}e_{r,p}(t) + \mathcal{C}x(t - \mu_{r,p}(t))) - K\Gamma^y(t_{r,p}h)\kappa^y(t_{r,p}h)$ for $t \in L_{r,p} \cap \Delta_{1,p}$. If not, the communication channel considered in this article is blocked, then $u(t) = 0$ for $t \in \Delta_{2,p}$.

Then, by combining (1) with (11), the dynamic model of the researched system can be depicted as follows:

$$\begin{cases} \dot{x}(t) = \begin{cases} \mathcal{A}x(t) - \mathcal{B}K[\mathcal{C}e_{r,p}(t) + \mathcal{C}x\big(t - \mu_{r,p}(t)\big) \\ +\Gamma^y\big(t_{r,p}h\big)\kappa^y\big(t_{r,p}h\big)] + \mathcal{F}\omega(t),\ t \in \Theta_1 \\ \mathcal{A}x(t) + \mathcal{F}\omega(t),\ t \in \Delta_{2,p} \end{cases} \\ y(t) = \mathcal{C}x(t),\ t \in \Theta_2 \end{cases} \tag{12}$$

where $\Theta_1 = L_{r,p} \cap \Delta_{1,p}$ and $\Theta_2 = (L_{r,p} \cap \Delta_{1,p}) \cup \Delta_{2,p}$.

Before addressing the problems presented in this article, an assumption, two definitions, and two lemmas are provided to deduce the desired results.

Assumption 1 [35]: A nonlinear function $\kappa(t)$, which is employed to restrain FDI attacks, meets the condition given as follows:

$$\|\kappa(t)\|^2 \le \|Hy(t)\|^2 \tag{13}$$

where H denotes a known matrix indicating an upper bound of nonlinear function $\kappa(t)$.

Definition 1 [36]: When $\omega(t) \equiv 0$, system (12) is exponentially mean-square stable (EMSS) if there are any two scalars $\varrho > 0$ and $\varpi > 0$ so that $\mathbb{E}\{\|x(t)\|^2\} \le \varrho\mathbb{E}\{\|x(t_0)\|^2\}e^{-\varpi t}$ holds for $\forall t \ge 0$.

Definition 2 [37]: For any nonzero $\omega(t) \in \mathcal{L}_2[0, \infty)$ and a predetermined positive scalar γ, system (12) is EMSS with an $\mathcal{H}_\infty$ performance if the following condition holds under zero-initial conditions:

$$\int_0^\infty \mathbb{E}\big\{y^T(s)y(s)\big\}ds \le \gamma^2 \int_0^\infty \omega^T(s)\omega(s)ds. \tag{14}$$

Lemma 1 ([38]): Considering a prescribed matrix $V > 0$, for any continuously differentiable function $\chi(t)$ in $[a_1, a_2] \to \mathbb{R}^n$, the inequality shown below holds

$$\int_{a_1}^{a_2} \dot{\chi}^T(\upsilon)V\dot{\chi}(\upsilon)d\upsilon \ge \frac{1}{a_2 - a_1}\chi_1^T V\chi_1 + \frac{3}{a_2 - a_1}\chi_2^T V\chi_2$$

where

$$\chi_1 \triangleq \chi(a_2) - \chi(a_1)$$
$$\chi_2 \triangleq \chi(a_2) + \chi(a_1) - \frac{2}{a_2 - a_1}\int_{a_1}^{a_2} \chi(\upsilon)d\upsilon.$$

Lemma 2 [39]: For any two vectors ϑ_1 and ϑ_2 , a matrix $L \in \mathbb{R}^{n\times n}$, symmetric positive definite matrices $J_1 \in \mathbb{R}^{n\times n}$ and $J_2 \in \mathbb{R}^{n\times n}$, and $\begin{bmatrix} J_1 & L \\ * & J_2 \end{bmatrix} > 0$, as well as any scalar $0 < \iota < 1$, the following condition holds:

$$-\frac{1}{\iota}\vartheta_1^T J_1\vartheta_1 - \frac{1}{1-\iota}\vartheta_2^T J_2\vartheta_2 \le -\begin{bmatrix} \vartheta_1 \\ \vartheta_2 \end{bmatrix}^T \begin{bmatrix} J_1 & L \\ * & J_2 \end{bmatrix}\begin{bmatrix} \vartheta_1 \\ \vartheta_2 \end{bmatrix}.$$

III. Main Results

In this section, some criteria guaranteeing the stability for system (12) under hybrid cyber attacks are deduced by dynamic ETTS (10). Subsequently, according to the obtained stability conditions, the problem of $\mathcal{H}_\infty$ control is further explored. Furthermore, the controller gain can be also obtained in view of the $\mathcal{H}_\infty$ stability conditions.

For brevity, some symbolic definitions are provided as follows:

$$\xi_1(t) \triangleq \big[\xi_{11}^T(t)\ \xi_{12}^T(t)\ \xi_{13}^T(t)\big]^T$$
$$\xi_2(t) \triangleq \big[\xi_{21}^T(t)\ \xi_{22}^T(t)\big]^T$$
$$\xi_{11}(t) \triangleq \big[x^T(t)\ x^T\big(t - \mu_{r,p}(t)\big)\ x^T(t - d_M)\big]^T$$
$$\xi_{21}(t) \triangleq \big[x^T(t)\ x^T\big(t - \mu_{r,p}(t)\big)\ x^T(t - d_M)\big]^T$$
$$\xi_{13}(t) \triangleq \big[e_{r,p}^T(t)\mathcal{C}^T\ \kappa^{yT}\big(t_{r,p}h\big)\ \omega^T(t)\big]^T$$
$$\xi_{12}(t) \triangleq \begin{bmatrix} \frac{1}{\mu_{r,p}(t)}\int_{t-\mu_{r,p}(t)}^{t} x(\tilde{v})d\tilde{v} \\ \frac{1}{d_M-\mu_{r,p}(t)}\int_{t-d_M}^{t-\mu_{r,p}(t)} x(\tilde{v})d\tilde{v} \\ \frac{1}{d_M}\int_{t-d_M}^{t} x(\tilde{v})d\tilde{v} \end{bmatrix}$$
$$\xi_{22}(t) \triangleq \begin{bmatrix} \frac{1}{\mu_{r,p}(t)}\int_{t-\mu_{r,p}(t)}^{t} x(\tilde{v})d\tilde{v} \\ \frac{1}{d_M-\mu_{r,p}(t)}\int_{t-d_M}^{t-\mu_{r,p}(t)} x(\tilde{v})d\tilde{v} \\ \frac{1}{d_M}\int_{t-d_M}^{t} x(\tilde{v})d\tilde{v} \\ \omega(t) \end{bmatrix}$$
$$\Sigma_1 \triangleq \begin{bmatrix} \mathrm{diag}\{Z_1, 3Z_1\} & X \\ * & \mathrm{diag}\{Z_1, 3Z_1\} \end{bmatrix}$$
$$\Sigma_2 \triangleq \begin{bmatrix} \mathrm{diag}\{Z_2, 3Z_2\} & N \\ * & \mathrm{diag}\{Z_2, 3Z_2\} \end{bmatrix}$$

$$
\begin{aligned}
X &\triangleq \begin{bmatrix} X_1 & X_2 \\ X_3 & X_4 \end{bmatrix}, N \triangleq \begin{bmatrix} N_1 & N_2 \\ N_3 & N_4 \end{bmatrix} \\
g_{i,p} &\triangleq \begin{cases} (p-1)\mathcal{T}, & i=1 \\ (p-1)\mathcal{T}+\mathcal{T}_{\text{off}}, & i=2 \end{cases} \\
\Phi_1 &\triangleq \left[e_1^T - e_2^T \;\; e_1^T + e_2^T - 2e_4^T\right]^T \\
\Phi_2 &\triangleq \left[e_2^T - e_3^T \;\; e_2^T + e_3^T - 2e_5^T\right]^T \\
\Phi_3 &\triangleq \left[e_1^T - e_3^T \;\; e_1^T + e_3^T - 2e_6^T\right]^T \\
e_i &\triangleq \left[0_{n\times(i-1)n} \; I_n \; 0_{n\times(9-i)n}\right], i = 1, 2, \ldots, 9.
\end{aligned}
$$

A. Stability and $\mathcal{H}_\infty$ Performance Analysis

Theorem 1: For prescribed positive scalars η, α, $\tilde{\theta}$, φ_i, ζ_i, d_M, $\bar{\tau}$, $\mathcal{H}_\infty$ performance index γ, constant matrix H, and $\mathcal{I}_{\text{DoS}}(t)$ with known positive scalars $\mathcal{T}$ and $\mathcal{T}_{\text{off}}$, if there are matrices $P_i > 0$, $Q_i > 0$, $R_i > 0$, $Z_i > 0$ $(i = 1, 2)$, N, and X with suitable dimensions, so that the inequalities shown below hold

$$\Lambda_i \triangleq \begin{bmatrix} \Lambda_i^{11} & \Lambda_i^{12} \\ * & \Lambda_i^{22} \end{bmatrix} < 0 \tag{15}$$

$$\Sigma_1 > 0, \Sigma_2 > 0 \tag{16}$$

$$P_1 \le \zeta_2 P_2, P_2 \le \zeta_1 e^{2(\varphi_1+\varphi_2)d_M} P_1 \tag{17}$$

$$Q_i \le \zeta_{3-i} Q_{3-i}, Z_i \le \zeta_{3-i} Z_{3-i}, R_i \le \zeta_{3-i} R_{3-i} \tag{18}$$

$$
\begin{aligned}
0 < \varkappa = {} & 2\varphi_1 \mathcal{T}_{\text{off}} - 2\varphi_2(\mathcal{T} - \mathcal{T}_{\text{off}}) \\
& - 2(\varphi_1+\varphi_2)d_M - \ln(\zeta_1\zeta_2)
\end{aligned} \tag{19}
$$

where

$$
\begin{aligned}
\Lambda_1^{11} &\triangleq \begin{bmatrix} \Pi_1 & \Pi_2 \\ * & \Pi_3 \end{bmatrix}, \Pi_2 \triangleq \begin{bmatrix} -P_1\mathcal{B}K & -\bar{\tau}P_1\mathcal{B}K & P_1\mathcal{F} \\ \mathcal{C}^T H^T H & 0 & 0 \\ 0_{4\times1} & 0_{4\times1} & 0_{4\times1} \end{bmatrix} \\
\Lambda_2^{12} &\triangleq \begin{bmatrix} b\mathcal{A}^T Z_2 & b\mathcal{A}^T R_2 \\ 0_{5\times1} & 0_{5\times1} \\ b\mathcal{F}^T Z_2 & b\mathcal{F}^T R_2 \end{bmatrix}, \Lambda_1^{12} \triangleq \begin{bmatrix} \Pi_4 \\ 0_{4\times4} \\ \Pi_5 \end{bmatrix} \\
\Pi_4 &\triangleq \begin{bmatrix} b\mathcal{A}^T Z_1 & 0 & b\mathcal{A}^T R_1 & 0 \\ -b\mathcal{C}^T K^T \mathcal{B}^T Z_1 & 0 & -b\mathcal{C}^T K^T \mathcal{B}^T R_1 & 0 \end{bmatrix} \\
\Pi_{51} &\triangleq \begin{bmatrix} -bK^T\mathcal{B}^T Z_1 & 0 \\ -b\bar{\tau}K^T\mathcal{B}^T Z_1 & b\sigma K^T\mathcal{B}^T Z_1 \\ b\mathcal{F}^T Z_1 & 0 \end{bmatrix}, \Pi_5 \triangleq \begin{bmatrix} \Pi_{51}^T \\ \Pi_{52}^T \end{bmatrix}^T \\
\Pi_{52} &\triangleq \begin{bmatrix} -bK^T\mathcal{B}^T R_1 & 0 \\ -b\bar{\tau}K^T\mathcal{B}^T R_1 & b\sigma K^T\mathcal{B}^T R_1 \\ b\mathcal{F}^T R_1 & 0 \end{bmatrix} \\
\Pi_3 &\triangleq \text{diag}\left\{H^T H - \Omega, -I, -\gamma^2 I\right\} \\
\Lambda_1^{22} &\triangleq \text{diag}\{-Z_1, -Z_1, -R_1, -R_1\} \\
\Lambda_2^{22} &\triangleq \text{diag}\{-Z_2, -R_2\} \\
\Pi_1 &\triangleq \begin{bmatrix} \Pi_1^{11} & \Pi_1^{12} & \Pi_1^{13} & \Pi_1^{14} & \Pi_1^{15} & \Pi_1^{16} \\ * & \Pi_1^{22} & \Pi_1^{23} & \Pi_1^{24} & \Pi_1^{25} & 0 \\ * & * & \Pi_1^{33} & \Pi_1^{34} & \Pi_1^{35} & \Pi_1^{36} \\ * & * & * & \Pi_1^{44} & \Pi_1^{45} & 0 \\ * & * & * & * & \Pi_1^{55} & 0 \\ * & * & * & * & * & \Pi_1^{66} \end{bmatrix}
\end{aligned}
$$

$$
\Lambda_2^{11} \triangleq \begin{bmatrix} \Pi_2^{11} & \Pi_2^{12} & \Pi_2^{13} & \Pi_2^{14} & \Pi_2^{15} & \Pi_2^{16} & \Pi_2^{17} \\ * & \Pi_2^{22} & \Pi_2^{23} & \Pi_2^{24} & \Pi_2^{25} & 0 & 0 \\ * & * & \Pi_2^{33} & \Pi_2^{34} & \Pi_2^{35} & \Pi_2^{36} & 0 \\ * & * & * & \Pi_2^{44} & \Pi_2^{45} & 0 & 0 \\ * & * & * & * & \Pi_2^{55} & 0 & 0 \\ * & * & * & * & * & \Pi_2^{66} & 0 \\ * & * & * & * & * & * & \Pi_2^{77} \end{bmatrix}
$$

with

$$
\begin{aligned}
\Pi_1^{11} &\triangleq 2\varphi_1 P_1 + \text{sym}\{P_1\mathcal{A}\} + Q_1 - 4a(Z_1 + R_1) + \mathcal{C}^T\mathcal{C} \\
\Pi_2^{16} &\triangleq 6\iota R_2, \Pi_2^{33} \triangleq -e^{2\varphi_2 d_M} Q_2 - \iota(4Z_2 + 4R_2) \\
\Pi_1^{12} &\triangleq -P_1\mathcal{B}K\mathcal{C} - a(2Z_1 + X_1 + X_2 + X_3 + X_4) \\
\Pi_1^{13} &\triangleq a(X_1 - X_2 + X_3 - X_4 - 2R_1), \Pi_1^{14} \triangleq 6aZ_1 \\
\Pi_1^{22} &\triangleq a(-8Z_1 + \text{sym}\{X_1 + X_2 - X_3 - X_4\}) + \mathcal{C}^T H^T H\mathcal{C} \\
&\quad + \eta(1+\alpha)\mathcal{C}^T\Omega\mathcal{C}, \Pi_1^{15} \triangleq 2a(X_2 + X_4) \\
\Pi_1^{23} &\triangleq a(-2Z_1 - X_1 + X_2 + X_3 - X_4), \Pi_1^{16} \triangleq 6aR_1 \\
\Pi_1^{24} &\triangleq a\left(6Z_1 + 2X_3^T + 2X_4^T\right), \Pi_2^{14} \triangleq 6\iota Z_2 \\
\Pi_1^{25} &\triangleq a(6Z_1 - 2X_2 + 2X_4), \Pi_2^{35} \triangleq 6\iota Z_2, \Pi_2^{17} \triangleq P_2\mathcal{F} \\
\Pi_1^{33} &\triangleq -e^{-2\varphi_1 d_M} Q_1 - a(4Z_1 + 4R_1), \Pi_1^{44} \triangleq -12aZ_1 \\
\Pi_1^{34} &\triangleq -2a\left(X_3^T - X_4^T\right), \Pi_1^{35} \triangleq 6aZ_1, \Pi_1^{36} \triangleq 6aR_1 \\
\Pi_1^{45} &\triangleq -4aX_4, \Pi_1^{55} \triangleq -12aZ_1, \Pi_1^{66} \triangleq -12aR_1 \\
\Pi_2^{11} &\triangleq -2\varphi_2 P_2 + \text{sym}\{P_2\mathcal{A}\} + Q_2 - 4\iota(Z_2 + R_2) \\
\Pi_2^{12} &\triangleq \iota(-2Z_2 - N_1 - N_2 - N_3 - N_4), \Pi_2^{66} \triangleq -12\iota R_2 \\
\Pi_2^{13} &\triangleq \iota(N_1 - N_2 + N_3 - N_4 - 2R_2), \Pi_2^{44} \triangleq -12\iota Z_2 \\
\Pi_2^{15} &\triangleq 2\iota(N_2 + N_4), \Pi_2^{34} \triangleq -2\iota\left(N_3^T - N_4^T\right) \\
\Pi_2^{22} &\triangleq \iota(-8Z_2 + \text{sym}\{N_1 + N_2 - N_3 - N_4\}) \\
\Pi_2^{23} &\triangleq \iota(-2Z_2 - N_1 + N_2 + N_3 - N_4), \Pi_2^{36} \triangleq 6\iota R_2 \\
\Pi_2^{24} &\triangleq \iota\left(6Z_2 + 2N_3^T + 2N_4^T\right), \Pi_2^{45} \triangleq -4\iota N_4, \Pi_2^{77} \triangleq -\gamma^2 I \\
\Pi_2^{25} &\triangleq \iota(6Z_2 - 2N_2 + 2N_4), \Pi_2^{55} \triangleq -12\iota Z_2 \\
a &\triangleq \frac{e^{-2\varphi_1 d_M}}{d_M}, b \triangleq \sqrt{d_M}, \iota \triangleq \frac{1}{d_M}
\end{aligned}
$$

system (12) is EMSS with decay rate $\varpi = \varkappa/\mathcal{T}$ and satisfies a given $\mathcal{H}_\infty$ performance index γ.

Proof: The Lyapunov–Krasovskii functionals for system (12) are constructed as

$$
\begin{aligned}
V_{\Upsilon(t)}(t) = {} & x^T(t)P_{\Upsilon(t)}x(t) \\
& + \int_{t-d_M}^{t} x^T(\tilde{\nu})e^{2(-1)^{\Upsilon(t)}\varphi_{\Upsilon(t)}(t-\tilde{\nu})}Q_{\Upsilon(t)}x(\tilde{\nu})d\tilde{\nu} \\
& + \int_{-d_M}^{0}\int_{t+\vartheta}^{t} \dot{x}^T(\tilde{\nu})e^{2(-1)^{\Upsilon(t)}\varphi_{\Upsilon(t)}(t-\tilde{\nu})}Z_{\Upsilon(t)}\dot{x}(\tilde{\nu})d\tilde{\nu}d\vartheta \\
& + \int_{-d_M}^{0}\int_{t+\vartheta}^{t} \dot{x}^T(\tilde{\nu})e^{2(-1)^{\Upsilon(t)}\varphi_{\Upsilon(t)}(t-\tilde{\nu})}R_{\Upsilon(t)}\dot{x}(\tilde{\nu})d\tilde{\nu}d\vartheta
\end{aligned}
$$

where

$$\Upsilon(t) = \begin{cases} 1, & t \in L_{r,p} \cap \Delta_{1,p} \\ 2, & t \in \Delta_{2,p}. \end{cases}$$

Through taking derivation of $V_1(t)$ along the trajectories of system (12) for $t \in L_{r,p} \cap \Delta_{1,p}$ and expectation, with

$\dot{\mu}_{r,p}(t) = 1$, the following formula is easily got:

$$\begin{aligned}\mathbb{E}\{\dot{V}_1(t)\} \le\ & \mathbb{E}\{\mathrm{sym}\{x^T(t)P_1\dot{x}(t)\}\} + x^T(t)Q_1x(t)\\ & - x^T(t-d_M)e^{-2\varphi_1 d_M}Q_1x(t-d_M) - 2\mathbb{E}\{\varphi_1 V_1(t)\}\\ & + 2\varphi_1 x^T(t)P_1x(t) + \mathbb{E}\{\dot{x}^T(t)d_M(Z_1+R_1)\dot{x}(t)\}\\ & - \int_{t-d_M}^{t}\dot{x}^T(\tilde{v})e^{-2\varphi_1 d_M}Z_1\dot{x}(\tilde{v})d\tilde{v}\\ & - \int_{t-d_M}^{t}\dot{x}^T(\tilde{v})e^{-2\varphi_1 d_M}R_1\dot{x}(\tilde{v})d\tilde{v}. \quad (20)\end{aligned}$$

Since

$$\begin{aligned}& -\int_{t-d_M}^{t}\dot{x}^T(\tilde{v})e^{-2\varphi_1 d_M}Z_1\dot{x}(\tilde{v})d\tilde{v}\\ &= -\ e^{-2\varphi_1 d_M}\int_{t-\mu_{r,p}(t)}^{t}\dot{x}^T(\tilde{v})Z_1\dot{x}(\tilde{v})d\tilde{v}\\ &\quad -\ e^{-2\varphi_1 d_M}\int_{t-d_M}^{t-\mu_{r,p}(t)}\dot{x}^T(\tilde{v})Z_1\dot{x}(\tilde{v})d\tilde{v} \quad (21)\end{aligned}$$

one can obtain the following inequalities via Lemma 1:

$$\begin{aligned}& -\int_{t-\mu_{r,p}(t)}^{t}\dot{x}^T(\tilde{v})Z_1\dot{x}(\tilde{v})d\tilde{v}\\ &\le -\frac{1}{\mu_{r,p}(t)}\xi_1^T(t)\Phi_1^T\begin{bmatrix}Z_1 & 0\\ * & 3Z_1\end{bmatrix}\Phi_1\xi_1(t) \quad (22)\\ & -\int_{t-d_M}^{t-\mu_{r,p}(t)}\dot{x}^T(\tilde{v})Z_1\dot{x}(\tilde{v})d\tilde{v}\\ &\le -\frac{1}{d_M-\mu_{r,p}(t)}\xi_1^T(t)\Phi_2^T\begin{bmatrix}Z_1 & 0\\ * & 3Z_1\end{bmatrix}\Phi_2\xi_1(t) \quad (23)\\ & -\int_{t-d_M}^{t}\dot{x}^T(\tilde{v})e^{-2\varphi_1 d_M}R_1\dot{x}(\tilde{v})d\tilde{v}\\ &\le -\frac{e^{-2\varphi_1 d_M}}{d_M}\xi_1^T(t)\Phi_3^T\begin{bmatrix}R_1 & 0\\ * & 3R_1\end{bmatrix}\Phi_3\xi_1(t). \quad (24)\end{aligned}$$

Afterwards, combining with (21)–(23) and Lemma 2, one has

$$\begin{aligned}& -\int_{t-d_M}^{t}\dot{x}^T(\tilde{v})e^{-2\varphi_1 d_M}Z_1\dot{x}(\tilde{v})d\tilde{v}\\ &\le -\frac{e^{-2\varphi_1 d_M}}{d_M}\xi_1^T(t)\begin{bmatrix}\Phi_1\\ \Phi_2\end{bmatrix}^T\Sigma_1\begin{bmatrix}\Phi_1\\ \Phi_2\end{bmatrix}\xi_1(t). \quad (25)\end{aligned}$$

For $t \in L_{r,p} \cap \Delta_{1,p}$, notice that

$$\dot{x}(t) = \left[A_0 - \left(\Gamma^y(t_{r,p}h) - \bar{\tau}\right)A_1\right]\xi_1(t)$$

where

$$A_0 = \mathcal{A}e_1 - \mathcal{B}K\mathcal{C}e_2 - \mathcal{B}Ke_7 - \bar{\tau}\mathcal{B}Ke_8 + \mathcal{F}e_9, A_1 = \mathcal{B}Ke_8.$$

Moreover, $\mathbb{E}\{\Gamma^y(t_{r,p}h) - \bar{\tau}\} = 0$ and $\mathbb{E}\{(\Gamma^y(t_{r,p}h) - \bar{\tau})^2\} = \sigma^2$. Consequently, we have

$$\begin{aligned}& \mathbb{E}\{\dot{x}^T(t)d_M(Z_1+R_1)\dot{x}(t)\}\\ &= \xi_1^T(t)\left(A_0^Td_M(Z_1+R_1)A_0 + A_1^T\sigma^2 d_M(Z_1+R_1)A_1\right)\xi_1(t). \quad (26)\end{aligned}$$

By recalling inequality (10), it can be obtained that

$$\begin{aligned}0 <\ & \Psi(t)x^T\left(t-\mu_{r,p}(t)\right)\mathcal{C}^T\Omega\mathcal{C}x\left(t-\mu_{r,p}(t)\right)\\ & -\ e_{r,p}^T(t)\mathcal{C}^T\Omega\mathcal{C}e_{r,p}(t). \quad (27)\end{aligned}$$

Then, considering

$$\eta\left(1-\alpha\tanh\left(e_{r,p}^T(t)e_{r,p}(t) - \tilde{\theta}\right)\right) < \eta(1+\alpha) \quad (28)$$

it is easily deduced that

$$\begin{aligned}0 <\ & \eta(1+\alpha)x^T\left(t-\mu_{r,p}(t)\right)\mathcal{C}^T\Omega\mathcal{C}x\left(t-\mu_{r,p}(t)\right)\\ & -\ e_{r,p}^T(t)\mathcal{C}^T\Omega\mathcal{C}e_{r,p}(t). \quad (29)\end{aligned}$$

In accordance with Assumption 1, it yields that

$$y^T\left(t_{r,p}h\right)H^THy\left(t_{r,p}h\right) - \kappa^{yT}\left(t_{r,p}h\right)\kappa^y\left(t_{r,p}h\right) \ge 0 \quad (30)$$

where $y(t_{r,p}h)$ satisfies equality (9).

Afterwards, combining (20)–(30), it is easily derived

$$\begin{aligned}\mathbb{E}\{\dot{V}_1(t)\} \le\ & \xi_1^T(t)\Lambda_1^{11}\xi_1(t) - 2\varphi_1\mathbb{E}\{V_1(t)\} + \gamma^2\omega^T(t)\omega(t)\\ & +\ \xi_1^T(t)A_0^Td_M(Z_1+R_1)A_0\xi_1(t) - y^T(t)y(t)\\ & +\ \xi_1^T(t)A_1^T\sigma^2d_M(Z_1+R_1)A_1\xi_1(t). \quad (31)\end{aligned}$$

By utilizing the Schur complement, $\Lambda_1 < 0$ can ensure that

$$\mathbb{E}\{\dot{V}_1(t)\} + y^T(t)y(t) - \gamma^2\omega^T(t)\omega(t) \le -2\varphi_1\mathbb{E}\{V_1(t)\} \quad (32)$$

then, one can easily deduce that $\mathbb{E}\{\dot{V}_1(t)\} \le -2\varphi_1\mathbb{E}\{V_1(t)\}$ holds when $\omega(t) \equiv 0$.

For $t \in \Delta_{2,p}$, by using the same processing method in $V_1(t)$ for $V_2(t)$, one has

$$\begin{aligned}\mathbb{E}\{\dot{V}_2(t)\} \le\ & \xi_2^T(t)\Lambda_2^{11}\xi_2(t) + \dot{x}^T(t)d_M(Z_2+R_2)\dot{x}(t)\\ & + 2\varphi_2\mathbb{E}\{V_2(t)\} + \gamma^2\omega^T(t)\omega(t) - y^T(t)y(t). \quad (33)\end{aligned}$$

Similarly, since $\Lambda_2 < 0$ and under the condition of $\omega(t) \equiv 0$, inequality $\mathbb{E}\{\dot{V}_2(t)\} \le 2\varphi_2\mathbb{E}\{V_2(t)\}$ holds.

Subsequently, we have

$$\mathbb{E}\{V(t)\} \le \begin{cases} e^{-2\varphi_1(t-g_{1,p})}\mathbb{E}\{V_1(g_{1,p})\}, & t \in [g_{1,p}, g_{2,p})\\ e^{2\varphi_2(t-g_{2,p})}\mathbb{E}\{V_2(g_{2,p})\}, & t \in [g_{2,p}, g_{1,p+1})\end{cases} \quad (34)$$

with $V(t) = V_{\Upsilon(t)}(t)$ and $\Upsilon(t) = 1, 2$. Based on conditions (17)–(19), the following inequalities can be got:

$$\begin{cases}\mathbb{E}\{V_1(g_{1,p})\} \le \zeta_2\mathbb{E}\left\{V_2\left(g_{1,p}^-\right)\right\}\\ \mathbb{E}\{V_2(g_{2,p})\} \le \zeta_1 e^{2(\varphi_1+\varphi_2)d_M}\mathbb{E}\left\{V_1\left(g_{2,p}^-\right)\right\}.\end{cases} \quad (35)$$

For $t \in [g_{1,p}, g_{2,p})$, from (34) and (35) and similar to [30], one has

$$\mathbb{E}\{V(t)\} \le e^{-\varkappa p}\mathbb{E}\{V_1(0)\}.$$

It is worth noting that $([t-\mathcal{T}_{\text{off}}]/\mathcal{T}) < p \le (t/\mathcal{T})$ can be deduced from $p\mathcal{T} = g_{1,p} \le t \le g_{2,p} = p\mathcal{T} + \mathcal{T}_{\text{off}}$. Consequently, one can derive that

$$\mathbb{E}\{V(t)\} \le e^{\frac{\varkappa\mathcal{T}_{\text{off}}}{\mathcal{T}}}e^{\frac{-\varkappa t}{\mathcal{T}}}\mathbb{E}\{V_1(0)\}. \quad (36)$$

In the same way, for $t \in [g_{2,p}, g_{1,p+1})$, one has

$$\mathbb{E}\{V(t)\} \le e^{\frac{-\varkappa t}{\mathcal{T}}}\mathbb{E}\{V_1(0)\}/\zeta_2. \quad (37)$$

Afterwards, define $\mathcal{G} \triangleq \max\{e^{\varkappa\mathcal{T}_{\text{off}}/\mathcal{T}}, (1/\zeta_2)\}$, $\mathcal{G}_1 \triangleq \min\{\lambda_{\min}(P_i)\}$, $\mathcal{G}_2 \triangleq \max\{\lambda_{\max}(P_i)\}$, $\mathcal{G}_3 \triangleq \mathcal{G}_2 + d_M\{\lambda_{\max}(Q_1)\} + (d_M^2/2)\lambda_{\max}(Z_1 + R_1)$, and $\varpi \triangleq \varkappa/\mathcal{T}$.

Then, according to (36) and (37), the inequality shown in the following can be gained

$$\mathbb{E}\{V(t)\} \le \mathcal{G}e^{\frac{-\varkappa t}{\mathcal{T}}}\mathbb{E}\{V_1(0)\} \quad \forall t \ge 0. \tag{38}$$

Furthermore, in accordance with the definition of $V(t)$, one has

$$\mathcal{G}_1\mathbb{E}\left\{\|x(t)\|^2\right\} \le \mathbb{E}\{V(t)\}, \mathbb{E}\{V_1(0)\} \le \mathcal{G}_3\mathbb{E}\left\{\|x(t_0)\|^2\right\}. \tag{39}$$

Thus, in terms of (38) and (39), for $\forall t \ge 0$, the following inequality can be achieved:

$$\mathbb{E}\left\{\|x(t)\|^2\right\} \le \frac{\mathcal{G}\mathcal{G}_3}{\mathcal{G}_1}e^{-\varpi t}\mathbb{E}\left\{\|x(t_0)\|^2\right\} \tag{40}$$

then, it indicates system (12) is EMSS with a decay rate ϖ.

By utilizing the Schur complement for inequality (31), the following inequality can be inferred:

$$\begin{aligned}&\mathbb{E}\left\{\dot{V}_1(t)\right\} + y^T(t)y(t) - \gamma^2\omega^T(t)\omega(t) + 2\varphi_1\mathbb{E}\{V_1(t)\}\\&\le \xi_1^T(t)\Lambda_1\xi_1(t).\end{aligned} \tag{41}$$

Hereafter, according to inequalities (15), (33), and (41), one has

$$\begin{aligned}&\mathbb{E}\left\{\dot{V}_i(t)\right\} - \gamma^2\omega^T(t)\omega(t) + y^T(t)y(t) + 2(-1)^{i+1}\varphi_i\mathbb{E}\{V_i(t)\}\\&\le 0, t \in \left[g_{i,p}, g_{3-i,p+i-1}\right).\end{aligned} \tag{42}$$

Under zero-initial conditions and referring to the proof in [30] and [40], for any $\omega(t) \in \mathcal{L}_2[0,\infty)$, integrating from 0 to $(p+1)\mathcal{T}$ on both sides of inequality (42), it yields that

$$\int_0^{(p+1)\mathcal{T}}\mathbb{E}\left\{y^T(t)y(t)\right\}dt - \gamma^2\int_0^{(p+1)\mathcal{T}}\omega^T(t)\omega(t)dt < 0.$$

When $p \to \infty$, one has

$$\int_0^{\infty}\mathbb{E}\left\{y^T(t)y(t)\right\}dt < \gamma^2\int_0^{\infty}\omega^T(t)\omega(t)dt \tag{43}$$

which implies that system (12) is EMSS with decay rate $\varpi = \varkappa/\mathcal{T}$ and a prescribed $\mathcal{H}_\infty$ performance index γ. This accomplishes the proof. ∎

B. Controller Design

Theorem 2: For several constant matrices H, S, Y_1, and Y_2 with suitable dimensions, and $\mathcal{I}_{\mathrm{DoS}}(t)$ with known positive scalars $\mathcal{T}$ and $\mathcal{T}_{\mathrm{off}}$, given positive scalars η, α, $\tilde{\theta}$, φ_i, ζ_i, d_M, $\bar{\tau}$, and $\mathcal{H}_\infty$ performance index γ, system (12) is EMSS with decay rate ϖ and a known $\mathcal{H}_\infty$ performance level γ, if there are matrices $P_i > 0$, $Q_i > 0$, $R_i > 0$, $Z_i > 0$ $(i = 1, 2)$, X, N, G, and U with suitable dimensions, so that conditions (16)–(19) and the following inequalities hold:

$$\bar{\Lambda}_1 \triangleq \begin{bmatrix}\bar{\Lambda}_1^{11} & \bar{\Lambda}_1^{12} & \bar{\Lambda}_1^{13}\\ * & \Lambda_1^{22} & \bar{\Lambda}_1^{23}\\ * & * & \bar{\Lambda}_1^{33}\end{bmatrix} < 0 \tag{44}$$

$$\bar{\Lambda}_2 \triangleq \Lambda_2 \triangleq \begin{bmatrix}\Lambda_2^{11} & \Lambda_2^{12}\\ * & \Lambda_2^{22}\end{bmatrix} < 0 \tag{45}$$

where

$$\bar{\Lambda}_1^{11} \triangleq \begin{bmatrix}\bar{\Pi}_1 & \bar{\Pi}_2\\ * & \Pi_3\end{bmatrix}, \bar{\Lambda}_1^{12} \triangleq \begin{bmatrix}\bar{\Pi}_4\\ 0_{4\times 4}\\ \bar{\Pi}_5\end{bmatrix}$$

$$\bar{\Pi}_1 \triangleq \begin{bmatrix}\Pi_1^{11} & \bar{\Pi}_1^{12} & \Pi_1^{13} & \Pi_1^{14} & \Pi_1^{15} & \Pi_1^{16}\\ * & \Pi_1^{22} & \Pi_1^{23} & \Pi_1^{24} & \Pi_1^{25} & 0\\ * & * & \Pi_1^{33} & \Pi_1^{34} & \Pi_1^{35} & \Pi_1^{36}\\ * & * & * & \Pi_1^{44} & \Pi_1^{45} & 0\\ * & * & * & * & \Pi_1^{55} & 0\\ * & * & * & * & * & \Pi_1^{66}\end{bmatrix}$$

$$\bar{\Pi}_4 \triangleq \begin{bmatrix}b\mathcal{A}^TZ_1 & 0 & b\mathcal{A}^TR_1 & 0\\ -b\mathcal{C}^TU^TY_1^T & 0 & -b\mathcal{C}^TU^TY_2^T & 0\end{bmatrix}$$

$$\bar{\Pi}_5 \triangleq \begin{bmatrix}-bU^TY_1^T & 0 & -bU^TY_2^T & 0\\ -b\bar{\tau}U^TY_1^T & \sigma bU^TY_1^T & -b\bar{\tau}U^TY_2^T & \sigma bU^TY_2^T\\ b\mathcal{F}^TZ_1 & 0 & b\mathcal{F}^TR_1 & 0\end{bmatrix}$$

$$\bar{\Lambda}_{11}^{23} \triangleq \begin{bmatrix}0_{1\times 2} & Z_1\mathcal{B} - Y_1G & 0 & 0 & 0\\ 0_{1\times 2} & 0 & 0 & Z_1\mathcal{B} - Y_1G & 0\\ 0_{2\times 2} & 0_{2\times 1} & 0_{2\times 1} & 0_{2\times 1} & 0_{2\times 1}\end{bmatrix}$$

$$\bar{\Lambda}_{12}^{23} \triangleq \begin{bmatrix}0_{2\times 1} & 0_{2\times 1} & 0_{2\times 1} & 0_{2\times 1}\\ R_1\mathcal{B} - Y_2G & 0 & 0 & 0\\ 0 & 0 & R_1\mathcal{B} - Y_2G & 0\end{bmatrix}$$

$$\bar{\Lambda}_{11}^{13} \triangleq \begin{bmatrix}P_1\mathcal{B} - SG & 0 & 0 & 0 & 0_{1\times 3} & 0 & 0_{1\times 2}\\ 0 & -\mathcal{C}^TU^T & 0 & -b\mathcal{C}^TU^T & 0_{1\times 3} & -b\mathcal{C}^TU^T & 0_{1\times 2}\end{bmatrix}$$

$$\bar{\Lambda}_{21}^{13} \triangleq \begin{bmatrix}0 & -U^T & 0 & -bU^T & 0 & 0 & 0 & -bU^T & 0 & 0\\ 0 & -\bar{\tau}U^T & 0 & -b\bar{\tau}U^T & 0 & \sigma bU^T & 0 & -b\bar{\tau}U^T & 0 & \sigma bU^T\\ 0 & 0 & 0 & 0 & 0 & 0 & 0 & 0 & 0 & 0\end{bmatrix}$$

$$\bar{\Pi}_2 \triangleq \begin{bmatrix}-SU & \bar{\tau}SU & P_1\mathcal{F}\\ \mathcal{C}^TH^TH & 0 & 0\\ 0_{4\times 1} & 0_{4\times 1} & 0_{4\times 1}\end{bmatrix}, \bar{\Lambda}_1^{13} \triangleq \begin{bmatrix}\bar{\Lambda}_{11}^{13}\\ 0_{4\times 10}\\ \bar{\Lambda}_{21}^{13}\end{bmatrix}$$

$$\begin{aligned}\bar{\Lambda}_{11}^{33} \triangleq{}& \mathrm{diag}\{\varepsilon_1I - \mathrm{sym}\{G\}, -\varepsilon_1I, \varepsilon_2I - \mathrm{sym}\{G\},\\ & -\varepsilon_2I, \varepsilon_3I - \mathrm{sym}\{G\}, -\varepsilon_3I\}\end{aligned}$$

$$\bar{\Lambda}_1^{23} \triangleq \left[\bar{\Lambda}_{11}^{23}\ \bar{\Lambda}_{12}^{23}\right], \bar{\Lambda}_1^{33} \triangleq \mathrm{diag}\left\{\bar{\Lambda}_{11}^{33}, \bar{\Lambda}_{12}^{33}\right\}$$

$$\bar{\Lambda}_{12}^{33} \triangleq \mathrm{diag}\{\varepsilon_4I - \mathrm{sym}\{G\}, -\varepsilon_4I, \varepsilon_5I - \mathrm{sym}\{G\}, -\varepsilon_5I\}$$

$$\bar{\Pi}_1^{12} \triangleq -SU\mathcal{C} - a(2Z_1 + X_1 + X_2 + X_3 + X_4)$$

and other symbols are the same as the corresponding definitions given in Theorem 1. Meanwhile, the controller gain matrix can be achieved

$$K = G^{-1}U. \tag{46}$$

Proof: For handling the coupling terms $P_1\mathcal{B}K$, $Z_1\mathcal{B}K$ and $R_1\mathcal{B}K$ in Theorem 1, three constant matrices (S, Y_1, Y_2) with suitable dimensions and any two unknown matrices (G, U) with appropriate dimensions are introduced. Define $P_1\mathcal{B}K \triangleq (P_1\mathcal{B} - SG)G^{-1}U + SU$, $Z_1\mathcal{B}K \triangleq (Z_1\mathcal{B} - Y_1G)G^{-1}U + Y_1U$ and $R_1\mathcal{B}K \triangleq (R_1\mathcal{B} - Y_2G)G^{-1}U + Y_2U$. Then, replace the coupling terms $P_1\mathcal{B}K$, $Z_1\mathcal{B}K$, and $R_1\mathcal{B}K$ in the condition Λ_1 with $(P_1\mathcal{B} - SG)G^{-1}U + SU$, $(Z_1\mathcal{B} - Y_1G)G^{-1}U + Y_1U$ and $(R_1\mathcal{B} - Y_2G)G^{-1}U + Y_2U$, respectively. Subsequently, by utilizing $\tilde{A}\tilde{B}^T + \tilde{B}\tilde{A}^T \le \varepsilon\tilde{A}\tilde{A}^T + \varepsilon^{-1}\tilde{B}\tilde{B}^T$ for $\Lambda_1 < 0$, we can further obtain that

$$0 > \begin{bmatrix}\bar{\Lambda}_1^{11} & \bar{\Lambda}_1^{12}\\ * & \Lambda_1^{22}\end{bmatrix} + \varepsilon_1\tilde{A}_1\tilde{A}_1^T + \varepsilon_1^{-1}\tilde{B}_1\tilde{B}_1^T + \varepsilon_2\tilde{A}_2\tilde{A}_2^T$$

TABLE II
PARAMETERS OF SYSTEM (1)

Parameters	$M\,(s)$	D	R	$T_g\,(s)$	$T_{ch}\,(s)$	β
Area 1	10	1.0	0.05	0.1	0.3	21.0
Area 2	12	1.5	0.05	0.17	0.4	21.5
Area 3	12	1.8	0.05	0.20	0.35	21.8

$$+\ \varepsilon_2^{-1}\tilde{B}_2\tilde{B}_2^T+\varepsilon_3\tilde{A}_3\tilde{A}_3^T+\varepsilon_3^{-1}\tilde{B}_3\tilde{B}_3^T+\varepsilon_4\tilde{A}_4\tilde{A}_4^T$$
$$+\ \varepsilon_4^{-1}\tilde{B}_4\tilde{B}_4^T+\varepsilon_5\tilde{A}_5\tilde{A}_5^T+\varepsilon_5^{-1}\tilde{B}_5\tilde{B}_5^T \qquad (47)$$

where

$$\begin{aligned}
\tilde{A}_1^T &\triangleq \begin{bmatrix}((P_1\mathcal{B}-SG)G^{-1})^T & 0_{1\times 12}\end{bmatrix}\\
\tilde{A}_2^T &\triangleq \begin{bmatrix}0_{1\times 9} & ((Z_1\mathcal{B}-Y_1G)G^{-1})^T & 0_{1\times 3}\end{bmatrix}\\
\tilde{A}_3^T &\triangleq \begin{bmatrix}0_{1\times 10} & ((Z_1\mathcal{B}-Y_1G)G^{-1})^T & 0_{1\times 2}\end{bmatrix}\\
\tilde{A}_4^T &\triangleq \begin{bmatrix}0_{1\times 11} & ((R_1\mathcal{B}-Y_2G)G^{-1})^T & 0\end{bmatrix}\\
\tilde{A}_5^T &\triangleq \begin{bmatrix}0_{1\times 12} & ((R_1\mathcal{B}-Y_2G)G^{-1})^T\end{bmatrix}\\
\tilde{B}_1^T &\triangleq \begin{bmatrix}0 & -U\mathcal{C} & 0_{1\times 4} & -U & -\bar{\tau}U & 0_{1\times 5}\end{bmatrix}\\
\tilde{B}_2^T &\triangleq \tilde{B}_4^T \triangleq \begin{bmatrix}0 & -bU\mathcal{C} & 0_{1\times 4} & -bU & -b\bar{\tau}U & 0_{1\times 5}\end{bmatrix}\\
\tilde{B}_3^T &\triangleq \tilde{B}_5^T \triangleq \begin{bmatrix}0_{1\times 7} & \sigma bU & 0_{1\times 5}\end{bmatrix}.
\end{aligned}$$

After that, using $-G\varepsilon^{-1}G^T \leq \varepsilon I_{n\times n}-\mathrm{sym}\{G\}$ and the Schur complement to inequality (47), $\bar{\Lambda}_1<0$ can be satisfied. This completes the proof. ■

Remark 7: For $t\in[g_{1,p},g_{2,p})$, the information transmission is normal due to the sleep of the jamming signal, while the signal of DoS attacks is active in interval $t\in[g_{2,p},g_{1,p+1})$ such that the communication channel between the event generator and the PI controller is interrupted. Therefore, the PI controller is only functional when the jamming signal of DoS attacks is dormant.

IV. ONE CASE STUDY

A simulation example about the three-area power system is provided to expound on the availability of an $\mathcal{H}_\infty$ load frequency controller based on a dynamic ETTS under hybrid cyber attacks in this section.

Table II shows the parameters of system (1) referred to [30]. Besides, $T_{12}=0.1986$, $T_{13}=0.2148$, and $T_{23}=0.1830$. Furthermore, assume that $\mathcal{T}=5$ and $\mathcal{T}_{\mathrm{off}}=4.95$. Choose $\varphi_1=0.05$, $\varphi_2=0.16$, $\zeta_1=\zeta_2=1.01$, $d_M=0.01$, $\eta=0.0005$, $\alpha=15$, $\tilde{\theta}=2.1$, and the $\mathcal{H}_\infty$ performance index $\gamma=30$. Moreover, suppose that the expectation of the occurrence of FDI attacks and the nonlinear function adopted to restrict FDI attacks are taken as $\bar{\tau}=0.02$ and $\kappa^y(t_{r,p}h)=-H\tanh(y(t_{r,p}h))$, respectively, where condition (13) can be satisfied with $H=\mathrm{diag}\{H_1,H_2,H_3\}$ in which $H_1=\mathrm{diag}\{1/60,1/60\}$, $H_2=\mathrm{diag}\{1/80,1/80\}$, and $H_3=\mathrm{diag}\{1/40,1/40\}$.

Next, select initial state as

$$x(0)=\begin{bmatrix}x_1^T(0) & x_2^T(0) & x_3^T(0)\end{bmatrix}^T$$

with $x_\flat(t)=[0\ 0\ 0\ 0\ 0]^T$, $\flat=1,2,3$, and the external disturbance $\omega(t)=\left[(0.4/[1+t^2])\ (0.4/[1+t^2])\ (0.4/[1+t^2])\right]^T$.

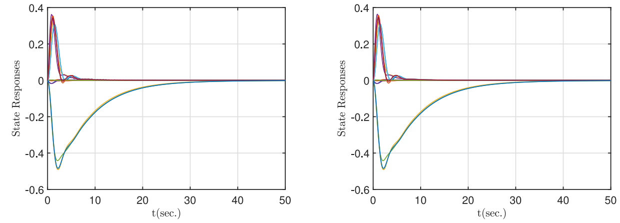

(a) (b)

Fig. 3. State responses of system (12) based on different ETTSs under hybrid cyber attacks. (a) State responses of system (12) with $\alpha=15$. (b) State responses of system (12) with $\alpha=0$.

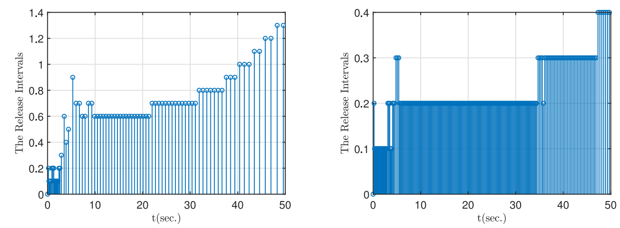

(a) (b)

Fig. 4. Release intervals based on different ETTSs under hybrid cyber attacks. (a) Release intervals under $\alpha=15$ and $\bar{\tau}=0.02$. (b) Release intervals under $\alpha=0$ and $\bar{\tau}=0.02$.

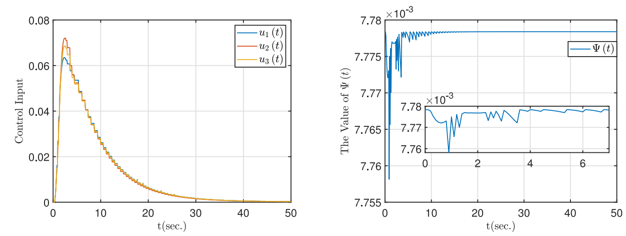

(a) (b)

Fig. 5. Other simulation results. (a) Input of PI controller (4) under $\alpha=15$ and $\bar{\tau}=0.02$. (b) Dynamic threshold function $\Psi(t)$ curve.

Then, on the basis of formula (46) in Theorem 2, the gain of the designed PI controller (4) is calculated as

$$K=\mathrm{diag}\{K_1,K_2,K_3\}$$

where

$$K_1=\begin{bmatrix}-0.0064 & 0.1436\end{bmatrix}, K_2=\begin{bmatrix}-0.0045 & 0.1469\end{bmatrix}$$
$$K_3=\begin{bmatrix}-0.0043 & 0.1419\end{bmatrix}.$$

Besides, in accordance with Theorem 2, the event-triggered weight matrix in condition (10) can be gotten as

$$\Omega=\mathrm{diag}\{\Omega_1,\Omega_2,\Omega_3\}$$

with

$$\Omega_1=\begin{bmatrix}413.4452 & 2.2818\\ 2.2818 & 119.9803\end{bmatrix}, \Omega_2=\begin{bmatrix}363.8067 & 1.2346\\ 1.2346 & 124.5780\end{bmatrix}$$
$$\Omega_3=\begin{bmatrix}359.6204 & 3.4369\\ 3.4369 & 106.9925\end{bmatrix}.$$

The simulation results obtained are presented in Figs. 3–5, respectively. Specifically, from Fig. 3(a) and (b), it can

Algorithm 1: Solving the Maximum Value of d_M

Input: Given some necessary system parameters;
Output: The maximum of d_M.
1 Give values for φ_1, φ_2, η, α, $\bar{\tau}$, γ, $\Delta\delta$, a search interval $[d_-, d_+]$ and $d_- \geq 0$;
2 Set $d = \frac{d_- + d_+}{2}$ and seek the solution to the conditions in Theorem 2;
3 **if** *the conditions in Theorem 2 are feasible* **then**
4   **if** $d - d_- \leq \Delta\delta$ **then**
5         $(d_M)_{\max} = d$;
6   go to 19;
7   **else**
8         $d_- = d$;
9   go back to 2;
10   **end**
11 **else**
12   **if** $d - d_- > \Delta\delta$ **then**
13         $d_+ = d$;
14   go to 2;
15   **else**
16   return to 1;
17   **end**
18 **end**
19 **return** $(d_M)_{\max}$.

be clearly seen that under the effect of the designed load frequency controller, the state trajectories of system (12) converge to zero, which fully proves the validity of the method proposed in this work. At the same time, in accordance with dynamic ETTS (10) subject to DoS attacks, the release intervals are drawn in Fig. 4(a). In particular, when $\alpha = 0$, dynamic ETTS (10) can be regarded as a static ETTS, and the release intervals are shown in Fig. 4(b). It is worth pointing out that the transmission rate (TR) of the sampled data is a momentous performance index to measure the ETTS, and the TRs of the dynamic ETTS and the static one are, respectively, 17% and 47.6% under the total number of the sampled data which is 500 during interval [0, 50 s] with the sampling period $h = 0.1$. Additionally, combining with Fig. 4(a) and (b) and TRs, we can see that the dynamic ETTS is more effective than the static one in reducing the number of data transmission and relieving the pressure of network communication to a greater extent under the same situation. Simultaneously, the input trajectories of PI controller (4) are displayed in Fig. 5(a), and the curve of the dynamic threshold function $\Psi(t)$ is displayed in Fig. 5(b). Furthermore, according to the above-mentioned parameters and conditions, the upper bound of time delays, which is introduced into system (12) by the dynamic ETTS and calculated by the dichotomy shown in Algorithm 1, can be gotten as $(d_M)_{\max} = 0.05$.

V. Conclusion

The problem of designing an $\mathcal{H}_\infty$ load frequency controller via a dynamic event-based scheme for multi-area power systems subject to FDI and DoS attacks has been addressed in this work. Under open network environments, a dynamic event-based scheme has been adopted to relieve the pressure of limited network bandwidth resources. Afterwards, sufficient conditions ensuring the exponential stability in the mean-square sense with $\mathcal{H}_\infty$ performance of the established system model have been deduced. Moreover, the desired controller gain has been obtained on the basis of the aforementioned series of work. Eventually, the usefulness of the proposed method has been verified via a simulation example. In future works, it is of great significance to generalize the proposed method to the observer-based extended dissipative aperiodic DoS attacks detection/defense problem, or to the distributed coordinated control of multiarea power systems with multiple time delays, referring to [41] and [42].

References

[1] H. Sun, C. Peng, D. Yue, Y. L. Wang, and T. Zhang, "Resilient load frequency control of cyber-physical power systems under QoS-dependent event-triggered communication," *IEEE Trans. Syst., Man, Cybern., Syst.*, vol. 51, no. 4, pp. 2113–2122, Apr. 2021.

[2] H. Zhang, J. Liu, and S. Xu, "H-infinity load frequency control of networked power systems via an event-triggered scheme," *IEEE Trans. Ind. Electron.*, vol. 67, no. 8, pp. 7104–7113, Aug. 2020.

[3] H. Shayeghi, H. A. Shayanfar, and A. Jalili, "Load frequency control strategies: A state-of-the-art survey for the researcher," *Energy Convers. Manag.*, vol. 50, no. 2, pp. 344–353, 2009.

[4] H. Bevrani and T. Hiyama, "Robust decentralised PI based LFC design for time delay power systems," *Energy Convers. Manag.*, vol. 49, no. 2, pp. 193–204, 2008.

[5] Ibraheem, P. Kumar, and D. P. Kothari, "Recent philosophies of automatic generation control strategies in power systems," *IEEE Trans. Power Syst.*, vol. 20, no. 1, pp. 346–357, Feb. 2005.

[6] X. Yu and K. Tomsovic, "Application of linear matrix inequalities for load frequency control with communication delays," *IEEE Trans. Power Syst.*, vol. 19, no. 3, pp. 1508–1515, Aug. 2004.

[7] C.-K. Zhang, L. Jiang, Q. Wu, Y. He, and M. Wu, "Delay-dependent robust load frequency control for time delay power systems," *IEEE Trans. Power Syst.*, vol. 28, no. 3, pp. 2192–2201, Aug. 2013.

[8] H. Zhang, J. H. Park, D. Yue, and W. Zhao, "Nearly optimal integral sliding-mode consensus control for multiagent systems with disturbances," *IEEE Trans. Syst., Man, Cybern., Syst.*, vol. 51, no. 8, pp. 4741–4750, Aug. 2021.

[9] L. Jiang, W. Yao, Q. H. Wu, J. Y. Wen, and S. J. Cheng, "Delay-dependent stability for load frequency control with constant and time-varying delays," *IEEE Trans. Power Syst.*, vol. 27, no. 2, pp. 932–941, May 2012.

[10] Ş. Sönmez, S. Ayasun, and C. O. Nwankpa, "An exact method for computing delay margin for stability of load frequency control systems with constant communication delays," *IEEE Trans. Power Syst.*, vol. 31, no. 1, pp. 370–377, Jan. 2016.

[11] S. Hu, D. Yue, X. Chen, Z. Cheng, and X. Xie, "Resilient H_∞ filtering for event-triggered networked systems under nonperiodic DoS jamming attacks," *IEEE Trans. Syst., Man, Cybern., Syst.*, vol. 51, no. 3, pp. 1392–1403, Mar. 2021.

[12] X.-M. Li, Q. Zhou, P. Li, H. Li, and R. Lu, "Event-triggered consensus control for multi-agent systems against false data-injection attacks," *IEEE Trans. Cybern.*, vol. 50, no. 5, pp. 1856–1866, May 2020.

[13] Z.-H. Pang, G.-P. Liu, D. Zhou, F. Hou, and D. Sun, "Two-channel false data injection attacks against output tracking control of networked systems," *IEEE Trans. Ind. Electron.*, vol. 63, no. 5, pp. 3242–3251, May 2016.

[14] G. Wu, J. Sun, and J. Chen, "Optimal data injection attacks in cyber-physical systems," *IEEE Trans. Cybern.*, vol. 48, no. 12, pp. 3302–3312, Dec. 2018.

[15] B. Niemoczynski, S. Biswas, and J. Kollmer, "Stability of discrete-time networked control systems under denial of service attacks," in *Proc. Resilience Week (RWS)*, Aug. 2016, pp. 119–124.

[16] C. Peng, J. Li, and M. Fei, "Resilient event-triggering H_∞ load frequency control for multi-area power systems with energy-limited DoS attacks," *IEEE Trans. Power Syst.*, vol. 32, no. 5, pp. 4110–4118, Sep. 2017.

[17] Z. Hu, S. Liu, W. Luo, and L. Wu, "Credibility-based secure distributed load frequency control for power systems under false data injection attacks," *IET Gener. Transm. Distrib.*, vol. 14, no. 17, pp. 3498–3507, 2020.

[18] E. Mousavinejad, F. Yang, Q.-L. Han, and L. Vlacic, "A novel cyber attack detection method in networked control systems," *IEEE Trans. Cybern.*, vol. 48, no. 11, pp. 3254–3264, Nov. 2018.

[19] B. Chen, D. W. C. Ho, W.-A. Zhang, and L. Yu, "Distributed dimensionality reduction fusion estimation for cyber-physical systems under DoS attacks," *IEEE Trans. Syst., Man, Cybern., Syst.*, vol. 49, no. 2, pp. 455–468, Feb. 2019.

[20] H. Yuan, Y. Xia, and H. Yang, "Resilient state estimation of cyber-physical system with multichannel transmission under DoS attack," *IEEE Trans. Syst., Man, Cybern., Syst.*, vol. 51, no. 11, pp. 6926–6937, Nov. 2021.

[21] G. Wu, G. Wang, J. Sun, and L. Xiong, "Optimal switching attacks and countermeasures in cyber-physical systems," *IEEE Trans. Syst., Man, Cybern., Syst.*, vol. 51, no. 8, pp. 4825–4835, Aug. 2021.

[22] H. Shen, M. Chen, Z.-G. Wu, J. Cao, and J. H. Park, "Reliable event-triggered asynchronous extended passive control for semi-Markov jump fuzzy systems and its application," *IEEE Trans. Fuzzy Syst.*, vol. 28, no. 8, pp. 1708–1722, Aug. 2020.

[23] Q. Zhang, H. Yan, H. Zhang, S. Chen, and M. Wang, "H_∞ control of singular system based on stochastic cyber-attacks and dynamic event-triggered mechanism," *IEEE Trans. Syst., Man, Cybern., Syst.*, vol. 51, no. 12, pp. 7510–7516, Dec. 2021.

[24] Z. Wu, Y. Wu, Z.-G. Wu, and J. Lu, "Event-based synchronization of heterogeneous complex networks subject to transmission delays," *IEEE Trans. Syst., Man, Cybern., Syst.*, vol. 48, no. 12, pp. 2126–2134, Dec. 2018.

[25] H. Sang and J. Zhao, "Input–output finite-time estimation for complex networks with switching topology under dynamic event-triggered transmission," *IEEE Trans. Syst., Man, Cybern., Syst.*, vol. 51, no. 10, pp. 6513–6522, Oct. 2021.

[26] H. Yan, Q. Yang, H. Zhang, F. Yang, and X. Zhan, "Distributed H_∞ state estimation for a class of filtering networks with time-varying switching topologies and packet losses," *IEEE Trans. Syst., Man, Cybern., Syst.*, vol. 48, no. 12, pp. 2047–2057, Dec. 2018.

[27] J. Dai and G. Guo, "Event-triggered leader-following consensus for multi-agent systems with semi-Markov switching topologies," *Inf. Sci.*, vol. 459, pp. 290–301, Aug. 2018.

[28] H. Yan, H. Zhang, F. Yang, X. Zhan, and C. Peng, "Event-triggered asynchronous guaranteed cost control for Markov jump discrete-time neural networks with distributed delay and channel fading," *IEEE Trans. Neural Netw. Learn. Syst.*, vol. 29, no. 8, pp. 3588–3598, Aug. 2018.

[29] M. Chen, H. Yan, H. Zhang, M. Chi, and Z. Li, "Dynamic event-triggered asynchronous control for nonlinear multiagent systems based on T–S fuzzy models," *IEEE Trans. Fuzzy Syst.*, vol. 29, no. 9, pp. 2580–2592, Sep. 2021.

[30] J. Liu, Y. Gu, L. Zha, Y. Liu, and J. Cao, "Event-triggered H_∞ load frequency control for multiarea power systems under hybrid cyber attacks," *IEEE Trans. Syst., Man, Cybern., Syst.*, vol. 49, no. 8, pp. 1665–1678, Aug. 2019.

[31] M.-F. Ge, Z.-W. Liu, G. Wen, X. Yu, and T. Huang, "Hierarchical controller-estimator for coordination of networked Euler–Lagrange systems," *IEEE Trans. Cybern.*, vol. 50, no. 6, pp. 2450–2461, Jun. 2020.

[32] J. Wang, C. Yang, J. Xia, Z.-G. Wu, and H. Shen, "Observer-based sliding mode control for networked fuzzy singularly perturbed systems under weighted try-once-discard protocol," *IEEE Trans. Fuzzy Syst.*, early access, Mar. 31, 2021, doi: 10.1109/TFUZZ.2021.3070125.

[33] H. Shen, M. Xing, H. Yan, and J. Cao, "Observer-based l_2–l_∞ control for singularly perturbed semi-Markov jump systems with improved weighted TOD protocol," *Sci. China Inf. Sci.*, to be published. [Online]. Available: https://www.sciengine.com/doi/10.1007/s11432-021-3345-1

[34] G. Liang, S. R. Weller, J. Zhao, F. Luo, and Z. Y. Dong, "The 2015 Ukraine blackout: Implications for false data injection attacks," *IEEE Trans. Power Syst.*, vol. 32, no. 4, pp. 3317–3318, Jul. 2017.

[35] J. Liu, E. Tian, X. Xie, and H. Lin, "Distributed event-triggered control for networked control systems with stochastic cyber-attacks," *J. Franklin Inst.*, vol. 356, no. 17, pp. 10260–10276, 2019.

[36] L. Su and H. Shen, "Mixed $\mathcal{H}_\infty$/passive synchronization for complex dynamical networks with sampled-data control," *Appl. Math. Comput.*, vol. 259, pp. 931–942, May 2015.

[37] H. Shen, X. Hu, J. Wang, J. Cao, and W. Qian, "Non-fragile H_∞ synchronization for Markov jump singularly perturbed coupled neural networks subject to double-layer switching regulation," *IEEE Trans. Neural Netw. Learn. Syst.*, early access, Sep. 6, 2021, doi: 10.1109/TNNLS.2021.3107607.

[38] A. Seuret and F. Gouaisbaut, "Wirtinger-based integral inequality: Application to time-delay systems," *Automatica*, vol. 49, no. 9, pp. 2860–2866, 2013.

[39] P. Park, J. W. Ko, and C. Jeong, "Reciprocally convex approach to stability of systems with time-varying delays," *Automatica*, vol. 47, no. 1, pp. 235–238, 2011.

[40] S. Hu, Y. Zhou, X. Chen, and Y. Ma, "H_∞ controller design of event-triggered networked control systems under quantization and denial-of-service attacks," in *Proc. IEEE 37th Chin. Control Conf.*, Wuhan, China, 2018, pp. 6338–6343.

[41] S. Hu, D. Yue, Z. Cheng, E. Tian, X. Xie, and X. Chen, "Co-design of dynamic event-triggered communication scheme and resilient observer-based control under aperiodic DoS attacks," *IEEE Trans. Cybern.*, vol. 51, no. 9, pp. 4591–4601, Sep. 2021.

[42] Z. Cheng, S. Hu, D. Yue, C. Dou, and S. Shen, "Resilient distributed coordination control of multiarea power systems under hybrid attacks," *IEEE Trans. Syst., Man, Cybern., Syst.*, vol. 52, no. 1, pp. 7–18, Jan. 2022.

Jing Wang received the Ph.D. degree in power system and automation from Hohai University, Nanjing, China, in 2019.

She is currently an Associate Professor with the Anhui University of Technology, Ma'anshan, China. Her current research interests include Markov jump nonlinear systems, singularly perturbed systems, power systems, and nonlinear control.

Dongji Wang received the B.Sc. degree in measurement and control technology and instrument from Maanshan University, Ma'anshan, China, in 2019. She is currently pursuing the M.S. degree with the School of Electrical and Information Engineering, Anhui University of Technology, Ma'anshan.

Her current research interests include power systems, event-triggered control, cyber attacks, and Markov jump systems.

Lei Su received the M.S. degree from the School of Electrical and Information Engineering, Anhui University of Technology, Ma'anshan, China, in 2016, and the Ph.D. degree in control theory and engineering from the Northeastern University, Shenyang, China, in 2020.

He is currently a Lecturer with the School of Electrical and Information Engineering, Anhui University of Technology. His research interests include fault-tolerant control, event-triggered control, Markov jump systems, and cyber–physical systems.

Ju H. Park (Senior Member, IEEE) received the Ph.D. degree in electronics and electrical engineering from the Pohang University of Science and Technology (POSTECH), Pohang, Republic of Korea, in 1997.

From May 1997 to February 2000, he was a Research Associate with Engineering Research Center-Automation Research Center, POSTECH. He joined Yeungnam University, Kyongsan, Republic of Korea, in March 2000, where he is currently the Chuma Chair Professor. He has coauthored the monographs *Recent Advances in Control and Filtering of Dynamic Systems With Constrained Signals* (New York, NY, USA: Springer-Nature, 2018) and *Dynamic Systems With Time Delays: Stability and Control* (New York, NY, USA: Springer–Nature, 2019) and is an Editor of an edited volume *Recent Advances in Control Problems of Dynamical Systems and Networks* (New York: Springer–Nature, 2020). His research interests include robust control and filtering, neural/complex networks, fuzzy systems, multiagent systems, and chaotic systems. He has published a number of articles in these areas.

Prof. Park has been a recipient of the Highly Cited Researchers Award by Clarivate Analytics (formerly, Thomson Reuters) since 2015 and listed in three fields, Engineering, Computer Sciences, and Mathematics, in 2019, 2020, and 2021. He also serves as an Editor of the *International Journal of Control, Automation and Systems*. He is also a Subject Editor/Advisory Editor/Associate Editor/Editorial Board Member of several international journals, including *IET Control Theory & Applications*, Applied Mathematics and Computation, Journal of The Franklin Institute, Nonlinear Dynamics, Engineering Reports, Cogent Engineering, the IEEE TRANSACTIONS ON FUZZY SYSTEMS, the IEEE TRANSACTIONS ON NEURAL NETWORKS AND LEARNING SYSTEMS, and the IEEE TRANSACTIONS ON CYBERNETICS. He is a Fellow of the Korean Academy of Science and Technology.

Hao Shen (Member, IEEE) received the Ph.D. degree in control theory and control engineering from the Nanjing University of Science and Technology, Nanjing, China, in 2011.

Since 2011, he has been with the Anhui University of Technology, Ma'anshan, China, where he is currently a Professor. His current research interests include stochastic hybrid systems, complex networks, fuzzy systems and control, and nonlinear control.

Prof. Shen was a recipient of the Highly Cited Researcher Award by Clarivate Analytics (formerly, Thomson Reuters) from 2019 to 2021. He has served on the technical program committee for several international conferences. He is an Associate Editor/Guest Editor for several international journals, including *Journal of the Franklin Institute*, *Applied Mathematics and Computation*, *Neural Processing Letters*, and *Transactions of the Institute Measurement and Control*.